Identification of Triple Flame Based on Numerical Data for Laminar Lifted Flames*

Susumu NODA** and Shuhei YAMAMOTO***

The flame base structures of laminar lifted flames are numerically investigated in order to develop a model of triple flame applicable to the flamelet model. The lifted flames formed in the downstream expanded duct developed by Kioni et al.[1] are calculated systematically in terms of the fuel concentration gradient at the inlet using a variant of the HSMAC method, modified so as to deal with variations of density. The triple flame is formed at the flame base of lifted nonpremixed flame for every case, even the case which does not initially have partial mixing. The diffusion flame appears to be supported by the enhancement of the surrounding premixed flames, resulting in a temperature rise. All scalar quantities along the premixed flames of the triple flame decline along a similar profile in mixture fraction space, and scalar quantities in the region surrounded by the premixed flames are almost completely conserved. On the basis of the results, we developed a model of triple flame that is applicable to the flamelet model. In the model, the region without reaction upstream of the flame base is referred to as the unburned region (frozen flow structure region), followed by the transition region outside the premixed flames, in which the flame changes from the frozen structure to the fully burning diffusion structure. The region surrounded by the premixed flames is referred to as the triple flame structure region. The region following the triple flame structure region is the fully burning diffusion flame structure region.

Key Words: Combustion Phenomena, Triple Flame, Lifted Flame, Flamelet Model, Simulation

1. Introduction

The liftoff of jet nonpremixed flames is an important flame characteristic and is related to flame instability or pollutant emission. In the proximal region between the nozzle rim and the flame base of lifted flame, fuel mixes partially with oxidizer; however, for turbulent lifted nonpremixed flames, there has been a long-standing controversy as to whether molecular premixing of the reactants is possible in such a short exposure time when the reactants are introduced separately[2]-[4]. It has been pointed out by Onuma et al.[5] that partial premixed combustion may be related to a reduction in NOx emission in turbulent lifted nonpremixed flames. Furthermore, laser diagnostics have revealed clear evidence of partial premixed combustion relating to triple flames in turbulent lifted nonpremixed flames[6]-[8]. Therefore, the analysis of triple flame, which originates around the flame base of turbulent lifted nonpremixed flame and consists of a rich and a lean premixed flames and a diffusion flame starting downstream from the triple point, may have the potential to improve the interpretation of turbulent nonpremixed flames.

Previous studies of triple flame have been focused on flame stability in the lifted state, because premixed flames have the propagation property. The research group of Chung at Seoul National University[9]-[13] found that triple flames are formed around flame bases of laminar lifted jet nonpremixed flames, and that liftoff heights can be predicted by jet theory, being based on the balance between flow and burning velocities. Buckmaster and Matalon[14] and Dold[15] theoretically investigated characteristics of triple flame, and the former found the flame geometry dependent on the Lewis number and the latter the relation between the propagation velocity and the mixture fraction gradient at leading edge of a triple flame. Muñiz and Mungal[16] found that turbulent lifted jet nonpremixed flames are stable at flame base locations for which the

* Received 7th December, 2005 (No. 05-4272)

** Department of Mechanical Engineering, Toyohashi University of Technology, 1–1 Hibarigaoka, Tempaku, Toyohashi 441–8580, Japan. E-mail: noda@mech.tut.ac.jp

*** Graduate Student, Department of Mechanical Engineering, Toyohashi University of Technology

flow velocity is less than three times the laminar burning velocity. Several researchers[1),(17)-(21)] reported that the flame propagation velocity is related to the fuel concentration gradient in the mixture. The relationship, however, is somewhat unclear due to an inconsistency in reported results; Phillips[17], Yamashita et al.[21] and Hirota et al.[19] reported a decrease in the propagation velocity with the fuel concentration gradient, while contradictory results are reported by Kioni et al.[1] Taking the geometry of the triple flame into consideration, which results in the creation of a low-velocity region immediately upstream of the tip of the flame as discussed in detail by Ruetsch et al.[20], the nominal propagation velocity may in fact increase with decreasing fuel concentration gradient up to the point at which geometry effects are no longer significant.

Müller et al.[22] developed the modified flamelet model using the scalar field variable G in order to predict turbulent lifted nonpremixed flames. In the model, the flame structure of the flame base is described simply as a weighted transitional structure between the frozen structure and the fully burning nonpremixed flame structure. As the structure is closely related to triple flame, the accuracy of the model depends strongly on the description of triple flame with respect to partial premixed combustion.

The objectives of the present study are to clarify the flame base structure of lifted nonpremixed flames and to develop a model of triple flame applicable to the estimation of turbulent lifted nonpremixed flames.

2. Nomenclature

C_{pi} : specific heat at constant pressure of species i
C_{pm} : mean specific heat at constant pressure
D : molecular diffusion coefficient
E : activation energy
h : specific enthalpy of mixture
h_i : specific enthalpy of species i
p : pressure
q : heat release rate
R_0 : universal gas constant
t : time
T : temperature
T_0 : standard-state temperature
u : x-directional velocity
u_S : burning velocity
v : y-directional velocity
W_i : molecular weight of species i
$\dot{w}_i$: rate of production of species i by chemical reactions
x : streamwise coordinate
y : lateral coordinate
$\bar{y}_C$: nondimensional combustible lateral width based on the duct width at the tip of the lifted flame
$\bar{Y}_C$: combustible fuel concentration width in terms of the mass fraction normalized by the stoichiometric value
Y_i : mass fraction of species i
Z : mixture fraction
Z_{st} : stoichiometric mixture fraction
ΔH_i^0 : heat of reaction at standard state of species i

Greek symbols

λ : thermal conductivity
μ : viscosity
ρ : density
ν_i' : stoichiometric coefficients of the reactant species i
ν_i'' : stoichiometric coefficients of the product species i

3. Formulation

3.1 Numerical configuration and calculation conditions

We numerically investigated laminar lifted flames formed in flow fields with fuel concentration gradients in a two-dimensional duct flow configuration expanded downstream to stabilize the flames, as depicted schematically in Fig. 1. This configuration was originally developed by Kioni et al.[1] and was continuously investigated by Kioni et al.[23] and also by Hirota et al.[18),(19)] The duct diverges at 4° downstream. The fuel is methane, the oxidizer is air, and the inflow velocity is adjusted so as to anchor a lifted flame in the duct. The boundary conditions employed in our calculations are listed in the figure and will be detailed later. The changes in flame base structure, giving the stoichiometric condition at the center line, were examined for a total of 8 inlet fuel concentration gradients (Fig. 2). The cases are denoted A to H; case A is a step-like distribution, with gradient decreasing to case H.

3.2 Formulation

Low Mach-number flow is considered. In the formulation, the following assumptions were employed in order to evaluate steady lifted flames: (1) the gas is ideal, (2) the Lewis number is unity, (3) the reaction of methane and

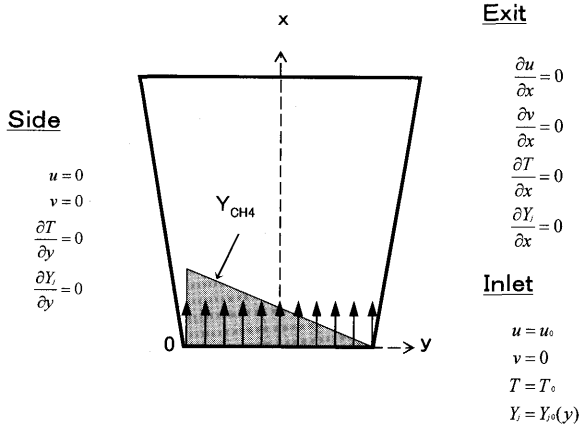

Fig. 1 Schematic of problem configuration and boundary conditions

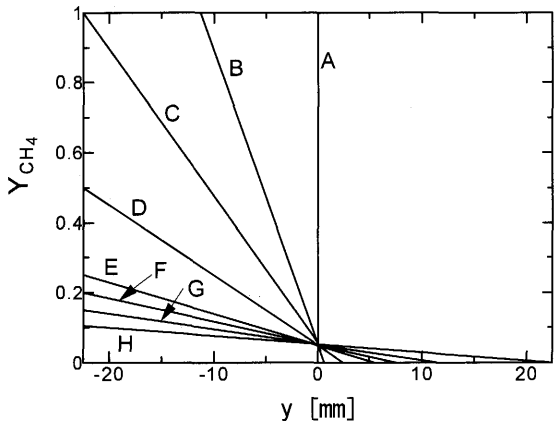

Fig. 2 Fuel concentration gradients at inlet for cases A to H. Stoichiometric condition is given at the center of the inlet

oxygen obeys a single-step, irreversible Arrhenius law, (4) the Soret and Dufour effects and the pressure gradient diffusion are negligible, (5) the thermal radiation and the bulk viscosity are negligible, and (6) the viscosity and the pressure fluctuation terms in the energy equation are negligible. Although steady-state solutions are sought, the time-derivative terms are retained in the equations because the numerical-solution algorithm adopted is based on a time-dependent approximation of a steady-state solution. The resulting governing equations are written as follows:

the continuity equation

$$\frac{\partial}{\partial t}\rho+\frac{\partial}{\partial x}(\rho u)+\frac{\partial}{\partial y}(\rho v)=0, \tag{1}$$

the x-momentum equation

$$\frac{\partial}{\partial t}(\rho u)+\frac{\partial}{\partial x}\left\{\rho u^2+p-\frac{2}{3}\mu\left(2\frac{\partial u}{\partial x}-\frac{\partial v}{\partial y}\right)\right\}+\frac{\partial}{\partial y}\left\{\rho uv-\mu\left(\frac{\partial u}{\partial y}+\frac{\partial v}{\partial x}\right)\right\}+\rho g=0, \tag{2}$$

the y-momentum equation

$$\frac{\partial}{\partial t}(\rho v)+\frac{\partial}{\partial x}\left\{\rho uv-\mu\left(\frac{\partial u}{\partial y}+\frac{\partial v}{\partial x}\right)\right\}+\frac{\partial}{\partial y}\left\{\rho v^2+p-\frac{2}{3}\mu\left(-\frac{\partial u}{\partial x}+2\frac{\partial v}{\partial y}\right)\right\}=0, \tag{3}$$

the species-mass equation

$$\frac{\partial}{\partial t}(\rho Y_i)+\frac{\partial}{\partial x}\left(\rho uY_i-\rho D\frac{\partial Y_i}{\partial x}\right)+\frac{\partial}{\partial y}\left(\rho vY_i-\rho D\frac{\partial Y_i}{\partial y}\right)=\dot{w}_i, \tag{4}$$

and the energy equation

$$\frac{\partial}{\partial t}(\rho h)+\frac{\partial}{\partial x}\left(\rho uh-\frac{\lambda}{C_{pm}}\frac{\partial h}{\partial x}\right)+\frac{\partial}{\partial y}\left(\rho vY_i-\frac{\lambda}{C_{pm}}\frac{\partial h}{\partial y}\right)=0. \tag{5}$$

Here, $\rho D=\lambda/C_{pm}$. Closure of the system of Eqs. (1)–(5) is achieved through the ideal-gas equation of state

$$\frac{p}{\rho}=R_0T\sum_{i=1}^{N}\left(\frac{Y_i}{W_i}\right). \tag{6}$$

Moreover, the mixture enthalpy h is related to temperature by its definition in terms of the species enthalpies, namely

$$h=\sum_{i=1}^{N}Y_ih_i, \tag{7}$$

where $h_i=\int_{T_o}^{T}C_{pi}dT+\Delta H_i^0$.

The source term in Eq. (4) is given by $\dot{w}_i=(\nu_i''-\nu_i')W_i\omega_i$. In the present work, we evaluate each $\dot{w}_i$ according to the reaction rate of methane $\omega_{CH4}=-AT^n\exp(-E/R_0T)(\rho Y_{CH4}/W_{CH4})^a(\rho Y_{O2}/W_{O2})^b$ proposed by Westbrook and Dryer[24], where $n=0$, $a=-0.3$, $b=1.3$, $A=1.3\times10^8\ \mathrm{s}^{-1}$, and $E=48.4$ kcal/mol. The reaction is also bounded in the combustible mixture between equivalence ratios of 0.5 and 1.6.

3.3 Numerical method

The governing equations are solved using the modified HSMAC method, which deals with variations in density[25], applying the first-order Euler method to the unsteady terms of the equations, the third-order up-wind scheme to the advective terms, and the second-order central scheme to the remainder. The computational space is divided by a staggered uniform spaced grid, obtained by transforming the non-uniform spaced grids of the diverged duct to the uniform grid according to a relation described in a textbook by Anderson et al.[26] The dimensions of the computational domain are 150 mm in the streamwise direction (x) and 45 mm in the lateral direction (y) at the inlet. The system is represented by a mesh system of $(x\times y)=(250\times150)$. A time increment of 20×10^{-6} s is employed for every calculation. The reaction is initiated by placing a Gaussian high-temperature source with maximum temperature of 2 000 K at a point 10 mm downstream of the inlet center, in the initial time interval.

It is necessary to establish suitable boundary conditions in order to obtain a numerical solution to the governing equations. At the duct inlet, the profiles of all variables are assumed to be known. The velocity is uniform, adjusted to around 0.15 m/s so as to suspend the flame in the duct during each calculation. Here, it should be noted that although the reaction rate formula employed in the present study gives correct burning velocities in the uniform mixtures[24], the propagation velocity of the triple flame is underestimated. This must lead to some deviations in terms of flame position. However, the scalar structure is more important for our subject to develop a model of triple flame. The present formula gives the flame temperature of approximately 2 300 K at the position of non-premixed flame as shown in Fig. 6 below against the stoichiometric flame temperature of 2 327 K estimated on the basis of the JANAF table[27]. This reveals that the formula

can adequately reproduce the scalar structure under the assumption of Lewis number of unity. Accordingly, we used the formula without modification because any modification would damage the validity of the results. The species mass fractions at the inlet are set on the basis of the fuel mass fraction profile for each case as mentioned above. The walls of the duct are dealt with as viscous boundaries. It is also assumed that the walls are adiabatic and impermeable to matter; the gradients of temperature and species mass fractions are therefore zero normal to each wall. The outflow from the duct is governed by the free flow-out condition, with the result that the gradients of all variables are zero in this region.

4. Results and Discussion

As explained in the introduction, we intend to establish a model of triple flame that is applicable for the estimation of turbulent lifted nonpremixed flames. Calculations were organized systematically from case A to H in order of decreasing fuel concentration gradient at the inlet. Figure 3 shows the distributions of temperature T and heat release rate q of steady lifted flames for cases B and F. Every flame contains the triple flame structure at the flame base, even case A (not shown here), which does not initially have partial mixing. Although the result for case A may suggest that the triple flame structure plays an important role in turbulent lifted nonpremixed flames, it should be pointed out that mixing occurs on the molecular level. In the present study, the mixing time turns out to be approximately 0.26 s, which is longer than that in turbulent lifted nonpremixed flames by a factor of hundred. Nevertheless, Schefer and Goix[6] and Watson et al.[7],[8] have revealed experimentally the existence of triple flame structures in turbulent lifted nonpremixed flames, indicating that partial premixing does occur under these conditions. The decreasing fuel concentration gradient at the inlet causes the wings of premixed flames to spread and activates the roles of the premixed flames, while weakening the diffusion flame, as indicated by a decrease in the heat release rate. This is a very natural phenomenon, because the decrease makes the initial premixed mixture uniform, leading to the normal premixed flame. It should be noted here that rich premixed wings are bent unnaturally, particularly for case F, as a result of the limitations regarding the combustible range applied in the reaction rate calculations. Preheat zones are apparent in all temperature distributions, with widths of less than 1 mm and located immediately upstream of the premixed flames. This is evidence that laminar lifted nonpremixed flames do not significantly affect the cold gas in the near field, as found in previous studies[9],[28]. The temperature distribution in the downstream region is approximately in parallel with the diffusion flame and exhibits diffusion dependence.

The tail of the rich premixed flame is longer than that of the lean premixed flame, and the most upstream position of flame is on the lean side in every case, as reported by Yamashita et al.[21], who employed skeletal chemistry for chemical kinetics[29]. The longer tail of rich premixed flame is attributed to the wider combustible physical space on the rich side compared to the lean side as a result of the linear concentration gradient set at the inlet, because the rich combustible range in terms of mass fraction is wider than the lean combustible range. The protrusion of premixed flame on the lean side is related to the longer rich premixed flame tail. This can be explained by velocity vector fields, as shown in Fig. 4. The flow is divergent immediately upstream of the flame tip, resulting in a low-velocity point and causing the flame to be shifted upstream, as documented in detail by Ruetsch et al.[20] and Yamashita et al.[21] Moreover, the mixture undergoes acceleration due to thermal expansion, passing through the premixed flames, as indicated clearly in case F (Fig. 4). This phenomenon is more prominent on the rich side because the combustible range is wider on the rich side, as

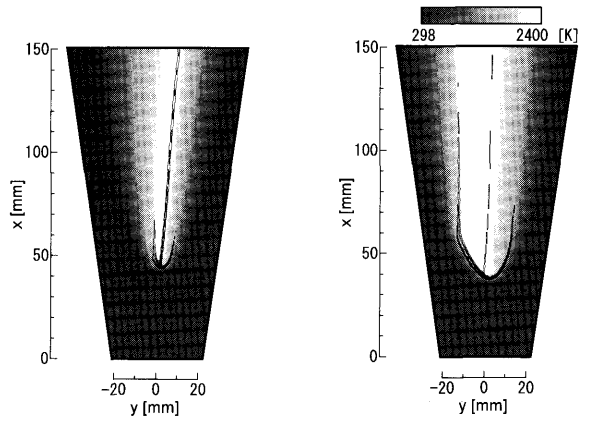

(a) Case B (b) Case F

Fig. 3 Temperature and heat release rate contours for cases B and F. Contour level q is $20\,\mathrm{MJ/m^3s} < q < 500\,\mathrm{MJ/m^3s}$ and interval is $\Delta q = 20\,\mathrm{MJ/m^3s}$

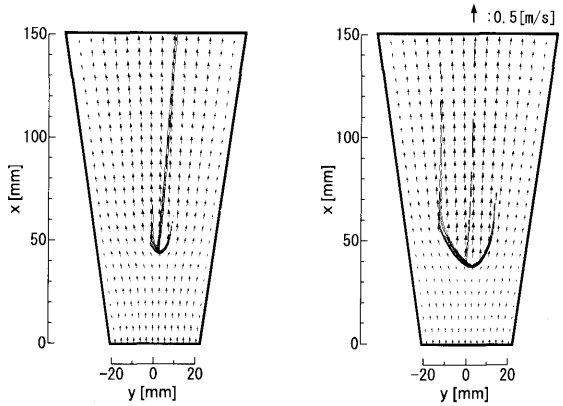

TypeB TypeF

Fig. 4 Velocity vector fields for cases B and F

mentioned above. This deforms the flame base toward the lean side; consequently, the most upstream tip of the triple flame shifts to the lean side. This result indicates that the triple point is not necessarily located at the upstream tip. In particular, in turbulent lifted flames, the flame bases are easily deformed by vortical motions. It is noticeable that our calculations have produced the phenomenon in which the velocity immediately upstream of the tip of the triple flame decreases due to the expansion of the flow field, while resembling the previous results obtained for the triple point[20)-(23)].

Figure 5 shows the burning velocity of the triple flame u_S as a function of the non-dimensional fuel concentration gradient $\bar{Y}_C/\bar{y}_C$. The burning velocity was measured immediately upstream of the tip of each triple flame. A decrease in fuel concentration gradient results in an increase in the burning velocity up to a peak followed by a rapid decrease. This tendency agrees well with an experimental result of Hirota et al.[19] and a numerical result of Yamashita et al.[21], however the burning velocity is underestimated by a factor of ten in this study, as a result of the reaction rate formula employed here. The increase in burning velocity is caused by the development of the triple flame with decreasing fuel concentration, which strengthens the reaction at the tip of the triple flame, as described later. We are unable to identify the cause of the rapid decrease in burning velocity at present, although it is expected to be related to the duct wall and the weakening of the diffusion flame.

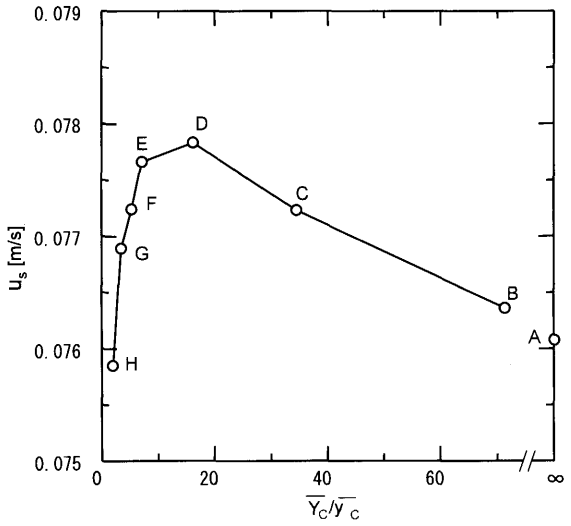

Fig. 5 Burning velocity as a function of the non-dimensional fuel concentration gradient

Figure 6 shows the temperature and heat release rate distributions for cases B and F across a cross-section 5 mm downstream of the triple point. Three peaks are apparent in each heat release rate distribution, corresponding to the rich premixed flame, the diffusion flame, and the lean premixed flame (from left to right in the figure). From the heat release rate distribution, the three flames are of equal strength for case B, whereas for case F, the decrease in the inlet fuel concentration gradient activates the premixed flames, with a corresponding reduction in the strength of the diffusion flame. The temperature is raised at the positions of the premixed flames, reaching the maximum temperature at the diffusion flame in our calculations.

Figure 7 shows the species concentration distributions for cases B and F across a cross-section 5 mm downstream of the triple point. Fuel and oxygen are consumed at the position of the premixed flame (Fig. 6), and excess reactants (fuel) on the rich side and oxidizer on the lean side diffuse to the diffusion flame to react between the rich and lean premixed flames. The products increase at the three flame positions. The decrease in the inlet fuel concentration gradient highlights the flame characteristic.

In order to further clarify the triple flame structure, the temperature and heat release rate distributions along the diffusion and premixed flames are shown in Figs. 8 and 9. Data for cases B, D, F, and H are used in the figures.

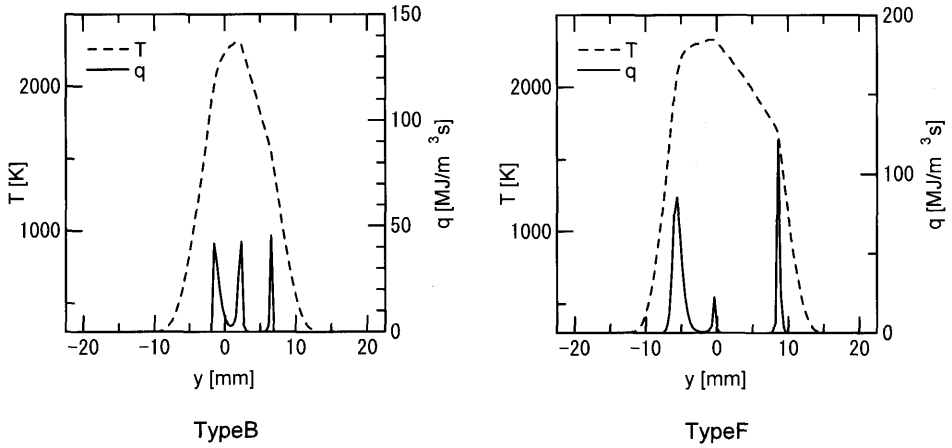

Fig. 6 Temperature and heat release rate distributions for cases B and F across a cross-section 5 mm downstream of the triple point

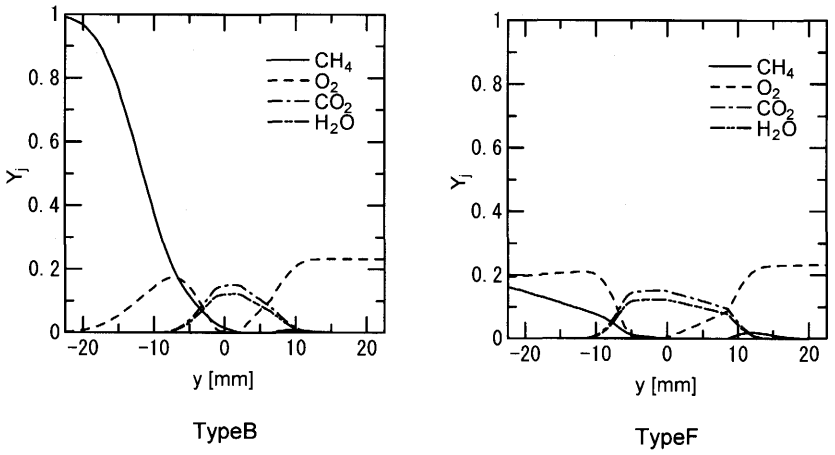

Fig. 7 Species concentration distributions for cases B and F across a cross-section 5 mm downstream of the triple point

The abscissa S_f indicates the distance along each flame from the triple point, with positive values indicating the lean side and negative values the rich side for premixed flames. For the diffusion flames (Fig. 8), the heat release rates take maximum values at the triple points, collapsing rapidly to lower values with increasing S_f. The relaxation of the inlet fuel concentration gradient reduces the heat release rate due to reduction in the supply of reactants to the diffusion flame. In contrast, temperature tends to increase, related to the shifting of temperature due to the activation of premixed flames (Fig. 6). The other noticeable point is that the triple point does not take the maximum temperature. The flame base diffuses the heat in all downward directions; the temperature at the end of the diffusion flame is therefore reduced. This phenomenon is also seen in the flame bases of lifted nonpremixed flames without triple flame[30]. The heat release rates along the premixed flames (Fig. 9) reveal a specific feature in that the peak points correspond to the most upstream positions of the triple flames, not the triple point. This is attributable to the flame geometry, by which the most upstream position of the triple flame is formed on the lean side, focusing the reactants at that point through the diffusion process and enhancing the reaction. This increases the temperature on the lean side with the growth of the triple flame, as shown in Fig. 9 (a), but not becomes maximum at the point. The heat release rates shown in Figs. 8 and 9 also reveal that main reaction of lifted nonpremixed flame occurs at the flame base.

The temperature, heat release rate and product concentration Y_{pro} distributions in the mixture fraction space are used to further clarify the triple flame structure. Figure 10 shows the temperature and heat release rate distributions along the premixed flames. The heat release rate peaks at a lean mixture fraction of approximately 0.046. Temperature, on the other hand, does not take a maximum at the corresponding value; rather, the peak temperature

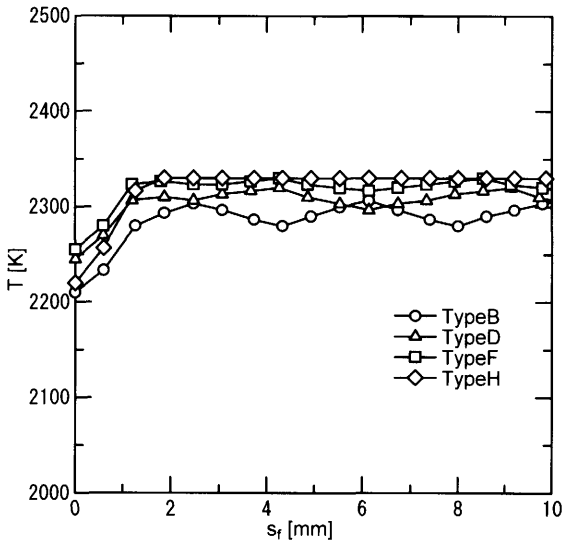

(a) Temperature

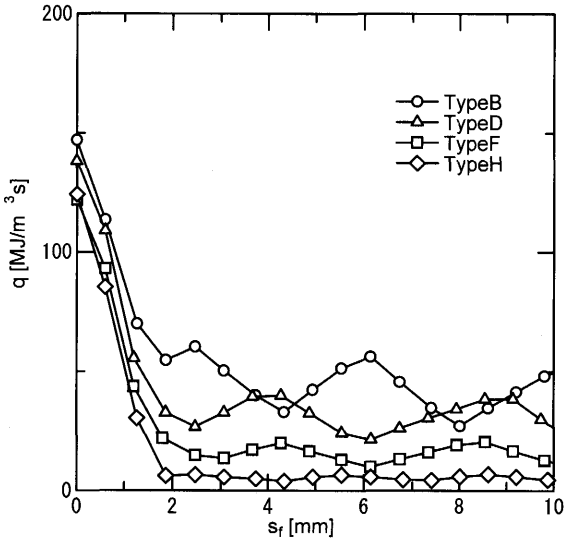

(b) Heat release rate

Fig. 8 Temperature and heat release rate distributions along diffusion flames for cases B, D, F and H. S_f is the distance from the triple point

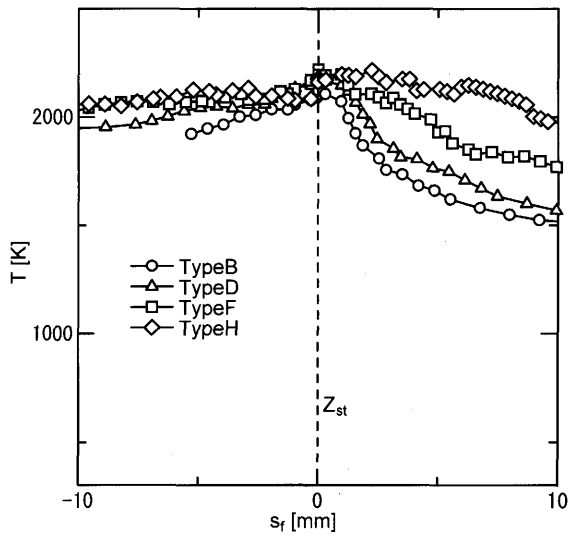

(a) Temperature

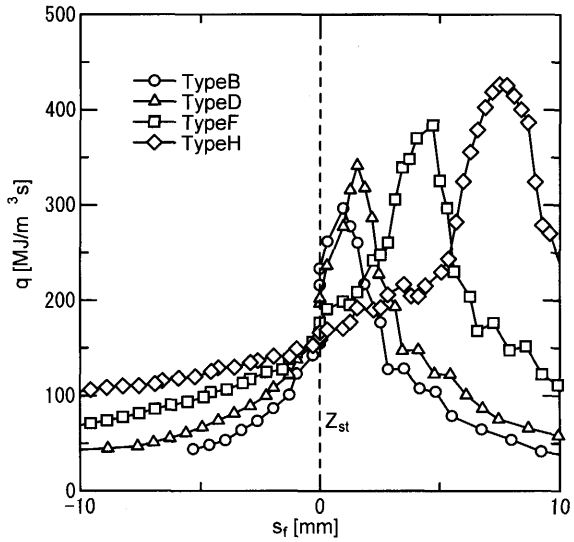

(b) Heat release rate

Fig. 9 Temperature and heat release rate distributions along premixed flames for cases B, D, F and H. S_f is the distance from the triple point; positive values indicate lean-side premixed flame and negative values indicate rich-side premixed flame

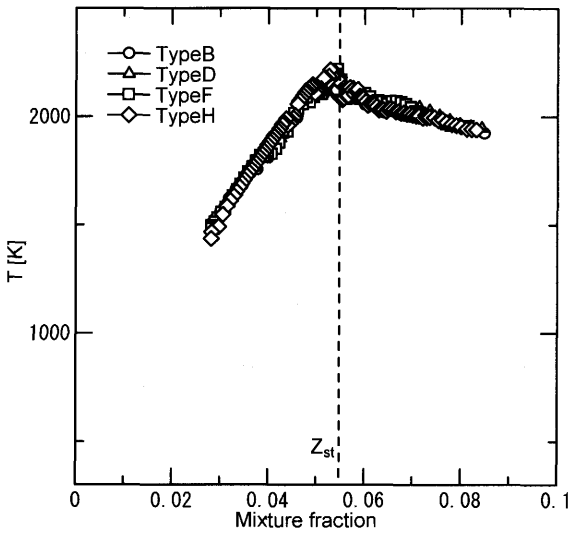

(a) Temperature

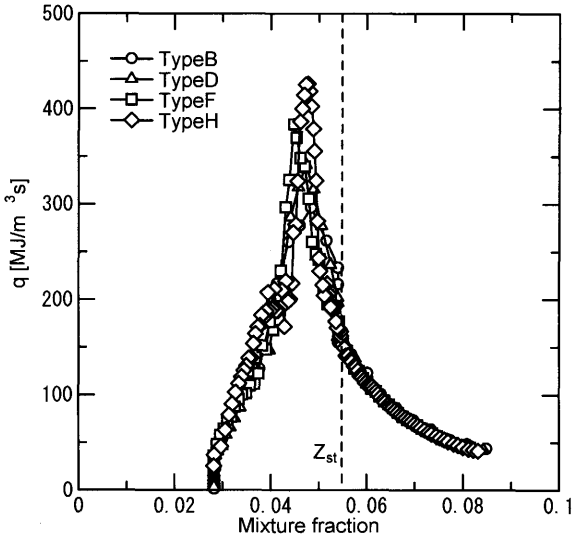

(b) Heat release rate

Fig. 10 Temperature and heat release rate distributions in mixture fraction space along premixed flames for cases B, D, F and H

occurs at very close to stoichiometry. The most important observation here is that all temperature data decreases along a similar profile, suggesting the possibility that a model of triple flame could be formed on this basis.

Figure 11 shows the temperature distributions in the mixture fraction space across a cross-section 5 mm downstream of the triple point for cases B, D, F, and H. Temperature takes a maximum at the stoichiometric mixture fraction of $Z = 0.054\,8$ for every flame. The temperature distributions in the region surrounded by the premixed flames gathers approximately around a line, with the temperature sifts at the positions of the premixed flames as indicated in Fig. 6. The temperature distributions can be interpreted as expressing the temperature field of the triple flame, because the cross-section is fixed 5 mm downstream of the triple point, even though the dimensions of the triple flames were changed by altering the inlet conditions. Consequently, it is also found that the temperature distribution in the region surrounded by the premixed flames is determined uniquely. Temperature distributions outside the triple flame are characteristic of transition profiles from the preheat structure to the fully burning diffusion flame structure, where case H corresponds to the upstream triple flame structure and case B is close to the fully burning diffusion flame structure.

These results also reveal that the scalar quantities in the region bounded by the premixed flames of the triple flame are almost completely conserved because temperature and species concentration (not shown here, because the distributions have the identical characteristic to those

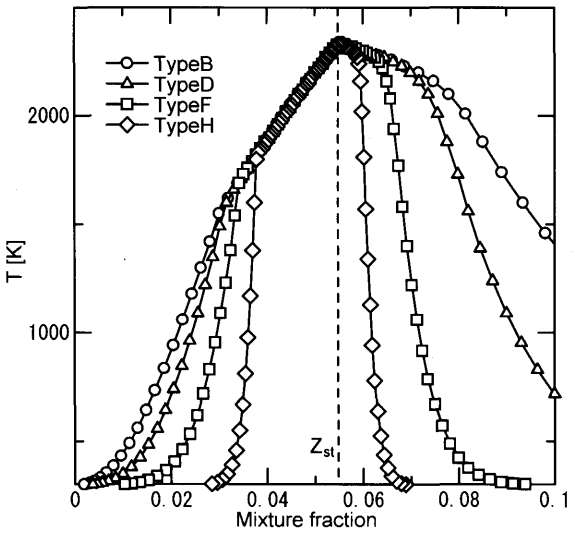

Fig. 11 Temperature distributions in mixture fraction space across a cross-section 5 mm downstream of the triple point, for cases B, D, F and H

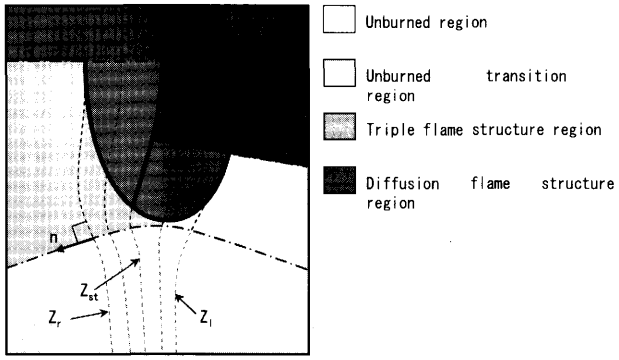

Fig. 12 Proposed flame base model

of temperature under the assumption of a Lewis number of unity) are uniquely determined in mixture fraction space. Main reaction occurs at the flame base of lifted nonpremixed flame as mentioned above. Therefore, this characteristic should be added to the flamelet model[22] with the scalar field equation for partially premixed combustion, for better estimation. A model developed from these observations is shown in Fig. 12. The region without reaction upstream of the flame base is referred to as the unburned region (frozen flow structure region), followed by the transition region outside the premixed flame, in which the flame changes from the frozen structure to the fully burning diffusion flame structure. The scalar structure of the transition region can be expressed in terms of the mixture fraction and a progress variable, described in detail elsewhere[31]. The region surrounded by the premixed flames is referred to as the triple flame structure region. The tail ends of the premixed flames may be determined for instance on the basis of the difference between the temperature along each premixed flame and that of the fully burning diffusion flame structure at the corresponding mixture fraction. The scalar quantities along the premixed flames are described in the mixture fraction space, as shown in Fig. 10. The values may be obtained by such ways as the equilibrium calculation or the counter flow calculation for premixed flames with various equivalence ratios. The scalar structure in the triple flame structure region can also be determined in other ways, including calculations of counterflow nonpremixed/partial premixed flames. The region downstream of the triple flame is the fully burning diffusion flame structure region, where the conventional flamelet model is applicable.

This triple flame model was derived on the basis of the one-step irreversible reaction model and the Lewis number of unity. However, these simple calculations extract the essence of the flame structure in an easy manner. The results are not dissimilar to the detailed triple flame calculations by Puri et al.[32] The proposed model is also expected to be applicable to turbulent lifted nonpremixed flame.

5. Conclusions

We have numerically examined the flame base structures of laminar lifted flames formed in duct flows with fuel concentration gradients in order to develop a model of triple flame applicable to flamelet model calculations of turbulent lifted nonpremixed flames. The results obtained are summarized as follows.

A decrease in the fuel concentration gradient at the inlet induces the development of premixed flames of the triple flame, as opening both the wings outside. The diffusion flame appears to be supported by the enhancement of the surrounding premixed flames, resulting in a temperature rise. The heat release rate was found to decrease with the fuel concentration gradient. The wing of the rich premixed flame becomes longer than of the lean premixed flame because the combustible physical space on the rich side is wider than on the lean side under the linear fuel concentration gradient at the inlet set in the present study. The longer rich premixed flame directs the velocity vectors toward the lean side, leading to a premixed flame geometry in which the flame tip is on the lean side.

All scalar quantities along the premixed flames of the triple flame decline along a similar profile in mixture fraction space, and scalar quantities in the region surrounded by the premixed flames are almost completely conserved. On the basis of the results, we developed a model of triple flame that is applicable to the flamelet model. In the model, the region without reaction upstream of the flame base is referred to as the unburned region (frozen flow structure region), followed by the transition region outside the premixed flames, in which the flame changes from the frozen structure to the fully burning diffusion structure. The region surrounded by the premixed flames is referred to as the triple flame structure region. The re-

gion following the triple flame structure region is the fully burning diffusion flame structure region. Modification of the model according to detailed chemical calculations will be addressed in future studies.

The authors are grateful for helpful discussions with Prof. Emeritus Y. Onuma.

References

(1) Kioni, P.N., Rogg, B., Bray, K.N.C. and Liñán, A., Flame Sread in Laminar Mixing Layers: The Triple Flame, Combust. Flame, Vol.95 (1993), pp.276–290.

(2) Vanquickenborn, L. and van Tiggelen, A., The Stabilization Mechanism of Lifted Diffusion Flames, Combust. Flame, Vol.10 (1966), pp.59–69.

(3) Kalghatgi, G.T., Blow-Out Stability of Gaseous Jet Diffusion Flames, Part 1, Still Air, Combust. Sci. Technol., Vol.26 (1981), pp.233–239.

(4) Peters, N. and Williams, F.A., Liftoff Characteristics of Turbulent Jet Diffusion Flames, AIAA J., Vol.21, No.3 (1983), pp.423–429.

(5) Onuma, Y., Yamauchi, T., Mawatari, M., Morikawa, M. and Noda, S., Low NOx Combustion by a Cyclone-Jet Combustor, JSME Int. J., Ser.B, Vol.44, No.2 (2001), pp.299–304.

(6) Schefer, R.W. and Goix, P.J., Mechanism of Flame Stabilization in Turbulent, Lifted-Jet Flames, Combust. Flame, Vol.112 (1998), pp.559–574.

(7) Watson, K.A., Lyons, K.M., Donbar, J.M. and Carter, C.D., Observation on the Leading Edge in Lifted Flame Stabilization, Combust. Flame, Vol.119 (1999), pp.199–202.

(8) Watson, K.A., Lyons, K.M., Donbar, J.M. and Carter, C.D., Simultaneous Rayleigh Imaging and CH-PLIF Measurements in a Lifted Jet Diffusion Flame, Combust. Flame, Vol.123 (2000), pp.252–265.

(9) Chung, S.H. and Lee, B.J., On the Characteristics of Laminar Lifted Flames in a Nonpremixed Jet, Combust. Flame, Vol.86 (1991), pp.62–72.

(10) Lee, B.J., Kim, J.S. and Chung, S.H., Effect of Dilution on the Liftoff of Nonpremixed Jet Flames, Proc. Combust. Inst., Vol.25 (1994), pp.1175–1181.

(11) Cha, M.S. and Chung, S.H., Characteristics of Lifted Flames in Nonpremixed Turbulent Confined Jets, Proc. Combust. Inst., Vol.26 (1996), pp.121–128.

(12) Lee, B.J., Cha, M.S. and Chung, S.H., Characteristics of Laminar Lifted Flames in a Partially Premixed Jet, Combust. Sci. Tech., Vol.127 (1997), pp.55–70.

(13) Lee, B.J. and Chung, S.H., Stabilization of Lifted Tribrachial Flames in a Laminar Nonpremixed Jet, Combust. Flame, Vol.109 (1997), pp.163–172.

(14) Buckmaster, J. and Matalon, M., Anomalous Lewis Number Effects in Tribrachial Flames, Proc. Combust. Inst., Vol.22 (1988), pp.1527–1535.

(15) Dold, J.W., Flame Propagation in a Nonuniform Mixture: Analysis of a Slowly Varying Triple Flame, Combust. Flame, Vol.76 (1989), pp.71–88.

(16) Muñiz, L. and Mungal, M.G., Instantaneous Flame-StabilizationVelocities in Lifted-Jet Diffusion Flames, Combust. Flame, Vol.111 (1997), pp.16–31.

(17) Phillips, H., Flame in a Buoyancy Methane Layer, Proc. Combust. Inst., Vol.10 (1965), pp.1277–1283.

(18) Hirota, M., Matsuo, A. and Mizomoto, M., Characteristics of Flame in Mixture with Concentration Gradient (1st Report), Thirty-Fifth Japanese Symp. Combust., (in Japanese), (1997), pp.564–566.

(19) Hirota, M., Matsuo, A. and Mizomoto, M., Characteristics of Flame in Mixture with Concentration Gradient (2nd Report), Thirty-Sixth Japanese Symp. Combust., (in Japanese), (1998), pp.404–405.

(20) Ruetsch, G.R., Vervisch, L. and Liñán, A., Effects of Heat Release on Triple Flames, Phys. Fluids, Vol.7, No.6 (1995), pp.1447–1454.

(21) Yamashita, H., Tutumitani, S. and Takeno, T., Effect of Concentration of Mixtures on the Flame Structure of Triple Flame, Thirty-Fourth Japanese Symp. Combust., (in Japanese), (1996), pp.225–227.

(22) Müller, C.M., Breitbach, H. and Peters, N., Partially Premixed Turbulent Flame Propagation in Jet Flames, Proc. Combust. Inst., Vol.25 (1994), pp.1099–1106.

(23) Kioni, P.N., Bray, K.N.C., Greenhalgh, D.A. and Rogg, R., Experimental and Numerical Studies of a Triple Flame, Combust. Flame, Vol.116 (1999), pp.192–206.

(24) Westbrook, C.K. and Dryer, F.L., Simplified Reaction Mechanisms for the Oxidation of Hydrocarbon Fuels in Flames, Combust. Sci. Technol., Vol.27 (1981), pp.31–43.

(25) Noda, S., Hashimoto, K. and Nakajima, T., Numerical Simulation of Growth of Flames Formed in a Two-Dimensional Mixing Layer (1st Report, Effect of Velocity ratios), Trans. Jpn. Soc. Mech. Eng., (in Japanese), Vol.60, No.572, B (1994), pp.1436–1442.

(26) Anderson, D.A., Tannehill, J.C. and Pletcher, R.H., Computational Fluid Mechanics and Heat Transfer, (1984), p.247, Hemisphere Publishing Corporation.

(27) Chase, M.W., Jr., NIST-JANAF Thermochemical Tables, Parts 1 and 2, 4th ed., (1988), Am. Chem. Soc.

(28) Noda, S., Makino, H. and Onuma, Y., Numerical Simulation of Growth of Flames Formed in a Two-Dimensional Mixing Layer (4th Report, Effects of Diffusion Flame on Mixing Layer), Trans. Jpn. Soc. Mech. Eng., (in Japanese), Vol.62, No.598, B (1996), pp.2452–2459.

(29) Smooke, M.D. and Giovangigli, V., Reduced Kinetic Mechanisms and Asymptotic Approximations for Methane-Air Flames, Edited by Smooke, M.D., (1991), Springer-Verlag.

(30) Takahashi, F., Schmoll, W.J. and Katta, V.R., Attachment Mechanism of Diffusion Flames, Proc. Combust. Inst., Vol.27 (1998), pp.675–684.

(31) Noda, S. and Tsubokura, T., Numerical Investigation of Edge Flame Structure of Counterflow Nonpremixed Flames with Local Extinction due to Flame Stretch, JSME Int. J., Ser.B, Vol.48, No.4 (2005), pp.849–857.

(32) Puri, I.K., Aggarwal, S.K., Ratti, S. and Azzoni, R., On the Similitude between Lifted and Burner-Stabilized Triple Flames: A Numerical and Experimental Investigation, Combust. Flame, Vol.124 (2001), pp.311–325.